Hindawi
BioMed Research International
Volume 2018, Article ID 8108713, 11 pages
https://doi.org/10.1155/2018/8108713

Research Article

A Novel Oxidovanadium (IV)-Orotate Complex as an Alternative Antidiabetic Agent: Synthesis, Characterization, and Biological Assessments

Ahmed M. Naglah,[1,2] **Mohamed A. Al-Omar**,[1] **Abdulrahman A. Almehizia**,[1,3] **Mashooq A. Bhat**,[3] **Walid M. Afifi**,[4] **Asma S. Al-Wasidi**,[5] **Jehan Y. Al-Humaidi**,[5] **and Moamen S. Refat**[6,7]

[1]*Department of Pharmaceutical Chemistry, Drug Exploration & Development Chair (DEDC), College of Pharmacy, King Saud University, Riyadh 11451, Saudi Arabia*
[2]*Peptide Chemistry Department, Chemical Industries Research Division, National Research Centre, 12622-Dokki, Cairo, Egypt*
[3]*Department of Pharmaceutical Chemistry, College of Pharmacy, King Saud University, Riyadh 11451, Saudi Arabia*
[4]*Department of Internal Medicine, Nephrology Unit, Faculty of Medicine, Zagazig University, Egypt*
[5]*Department of Chemistry, College of Science, Princess Nourah Bint Abdulrahman University, Riyadh 11671, Saudi Arabia*
[6]*Department of Chemistry, Faculty of Science, Taif University, P.O. Box 888, Al-Hawiah, Taif 21974, Saudi Arabia*
[7]*Department of Chemistry, Faculty of Science, Port Said University, Port Said, Egypt*

Correspondence should be addressed to Ahmed M. Naglah; anaglah@ksu.edu.sa

Received 30 October 2018; Revised 3 December 2018; Accepted 9 December 2018; Published 23 December 2018

Academic Editor: Swaran J. S. Flora

Diabetes is an increasingly common metabolic disorder with high comorbidity and societal and personal costs. Insulin replacement therapy is limited by a lack of oral bioavailability. Recent studies suggest vanadium has therapeutic potential. A newly synthesized complex between oxidovanadium (IV) and orotic acid (OAH_3), $[(OAH_1)(VO)(NH_3)_2].3H_2O$, was characterized using spectroscopic and thermogravimetric techniques. *In vivo* potential was assessed in a streptozocin-induced rat model of diabetes. OAH_3 acts as a bidentate ligand in the formation of the dark green, crystalline oxidovanadium (IV) complex in a square pyramidal configuration. Treatment with oxidovanadium (IV)-orotate *in vivo* significantly improved many biochemical parameters with minimal toxicity and restored pancreatic and hepatic histology. The results of the present work describe a safe, new compound for the treatment of diabetes.

1. Introduction

Metals represent approximately 0.03% of the total body mass and metal deficiencies can be deleterious (e.g., anemia, osteoporosis). Moreover, it has been reported that malignant tumors isolated from the kidney contain lower concentrations of Cd, Cr, Ti, V, Cu, Se, and Zn relative to noncancerous kidney tissue [1]. Both unbound and chelated metals have greatly contributed to the development and efficacy of chemotherapeutic agents [2]. These compounds are often administered as prodrugs, which have different physical and pharmacological properties compared to their metabolized active derivatives, and thus provide more control over the timing and location of the drug release [3]. For example, the complexation between nonsteroidal anti-inflammatory drugs and copper prevents some of the gastric side effects of these drugs [4]. The release of cytotoxins from redox-active metals (e.g., cobalt) is induced by the hypoxic microenvironment characteristic of solid tumors; this targeted release mechanism confers greater potency and incurs less collateral toxicity [5]. Moreover, the therapeutic application of metal ions is not limited to cancer but it also includes the treatment of diabetes and inflammatory and cardiovascular diseases [6].

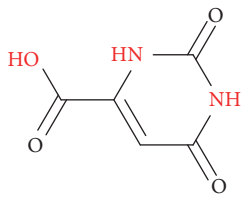

Figure 1: Chemical structure of orotic acid (OAH_3).

Many studies have described the ability of the metal vanadium (as ions and in complexes) to treat diabetes [7, 8] and fight cancer [9]. The latter has been attributed to vanadium's potent insulin-like effects in the liver, skeletal muscle, and adipose tissue [7]. Additionally, studies have shown that vanadium compounds can provide significant antioxidant effects both *in vitro* and *in vivo* [10]. However, vanadium (IV) and (V) salts are not easily absorbed in the gastrointestinal tract and have strong side effects, which were evidenced in the literature using biochemical assays [11]. Therefore, research efforts have been dedicated to the synthesis of novel vanadium compounds in complex with organic chelating ligands and the subsequent determination of their therapeutic potential using both cell-based and animal disease models [7]. Using these experimental approaches in addition to clinical trials on human subjects, vanadium compounds have been shown to improve the hyperglycemia characteristic of type-one diabetes as well as the glucose homeostasis in type 2 diabetes [12].

Vitamin B_{13} refers to orotic acid (OAH_3), which plays a fundamental role in the biosynthesis of nucleic acids, where it serves as a key precursor in the pyrimidine formation pathway in all living organisms [13].

The chemical structure of OAH_3 is illustrated in Figure 1. It exhibits multidentate functionality in transition metal complexes and plays an important role in bioinorganic chemistry. Metal orotates are widely applied in the field of medicine. Researchers have screened platinum, palladium, and nickel orotates with various substituent for therapeutic activity against cancer, and zinc (II) and cobalt (II) orotates are antimicrobial [14]. Metal orotates are cell-penetrable; therefore, they can be used to treat conditions associated with intracellular dysfunction (e.g., calcium, magnesium, zinc, or iron deficiency) [15]. Both OAH_3 and its Mg (II) salt have a beneficial effect in prophylaxis and diseases of the heart and vasculature [16]. The nutritional importance of OAH_3 lies in its role as a growth factor and as a protective agent in the liver [17]. OAH_3 improves the symptoms caused by folate and cobalamin deficiencies and increases intracellular levels of nucleotides and nucleic acids. Large doses of magnesium orotate (3 g/day) markedly improved left ventricular function and exercise tolerance in patients with coronary heart disease, likely by correcting nucleotide precursors deficiency or by increasing the myocardial energy supply [18]. OAH_3 has already been used clinically to treat neonatal jaundice [19], hyper lipoproteinemia [20], degenerative retinal disease [21], and gout [22].

Here we describe the synthesis and characterization of a novel oxidovanadium (IV)-orotate complex with potential therapeutic application to the treatment of diabetes, which was investigated using a streptozocin (STZ)-induced diabetes rat model.

2. Materials and Methods

2.1. Chemicals and Reagents. All chemicals and reagents used in this investigation were of the highest grading available (Aldrich) and employed without further purification. OAH_3 and oxidovanadium (IV) sulfate monohydrate were also procured from Aldrich Company.

2.2. Synthesis of the Oxidovanadium (IV)-Orotate Complex. The bidistilled water was employed as a solvent for the oxidovanadium (IV)-orotate complex. The $[(OAH_1)(VO)(NH_3)_2].3H_2O$ complex was synthesized using a 1:1 $VOSO_4$:OAH_3 ratio. $VOSO_4.H_2O$ (0.181 g, 1.0 mmol) salt was dissolved in aqueous media and then directly added to 40 mL of CH_3OH/H_2O OAH_3 (0.156 g, 1.0 mmol) solution. The CH_3OH/H_2O OAH_3 solution was pretitrated with 5% NH_3 to adjust to pH 9, then heated at ~60°C for 30 minutes until the precipitate settled, and left to evaporate at room temperature overnight. The precipitate was filtered, washed several times with minimal amounts of hot methanol, dried in an oven at 60°C, and then stored in a vacuum desiccator over anhydrous $CaCl_2$.

2.3. Instruments. Analyses of C, H, and N content (%) were performed using the Perkin Elmer CHN 2400 microanalysis unit. Vanadium metal content was determined gravimetrically by the direct ignition of the complex at 800°C for 3 hours until a constant mass was reached. The residue was then weighed in the form of vanadium oxide. The molar conductivity of freshly prepared 1.0×10^{-3}mol/cm^3 oxidovanadium (IV)-orotate complex dimethyl sulfoxide (DMSO) solution was measured using a JENWAY 4010 conductivity meter.

The solid reflectance spectrum was measured on a UV-3101 PC UV–Vis Spectrophotometer. The infrared spectra were recorded with KBr discs on a Bruker FT-IR Spectrophotometer (4000 – 400 cm^{-1}). Magnetic data were calculated at 25°C using Magnetic Susceptibility Balance (Sherwood Scientific, Cambridge, England) at Cairo University, Cairo, Egypt. The electronic paramagnetic resonance (EPR) spectrum was determined at 9.44 GHz using the JES-FE2XG EPR-spectrometer and microwave unit.

Thermal studies included thermogravimetric (TG), differential thermogravimetric (DTG), and differential thermal (DTA) analyses and were carried out on the Shimadzu Thermogravimetric Analyzer in atmospheric nitrogen, from room temperature up to 800°C. Scanning electron microscopy (SEM) images were acquired using the Quanta FEG 250 microscope. Transmission electron microscopy (TEM) images were acquired using the JEOL 100s microscope. The X-ray diffraction patterns were recorded on the X'Pert PRO PANalytical X-ray powder diffraction (XRD) unit using target copper with a secondary monochromate.

2.4. In Vivo Experimental Design. Male albino rats (100 - 120 g) were purchased from the National Research Centre (Cairo, Egypt). The animals were housed in solid-bottom polycarbonate cages with stainless steel wire-bar lids and wood-based dust-free litter as bedding material. They were allowed free access to food and kept in an air-conditioned room for two weeks prior to starting the experiment. All animal procedures were performed in accordance with the European Community Directive (86/609/EEC) and the National Rules on Animal Care.

The animals were divided into four groups of 10 animals per group:

(i) Group I: untreated negative control

(ii) Group II: untreated diabetic positive control: one-time intraperitoneal (i.p.) injection of STZ (50 mg/kg) [23]

(iii) Group III: oxidovanadium(IV) sulfate alone: one-time i.p. injection of STZ (50 mg/kg) followed by i.p. injections of oxidovanadium(IV) sulfate alone (40 mg/kg) every other day for 30 days (15 total treatments)

(iv) Group IV: the oxidovanadium (IV)-orotate complex: one-time i.p. injection of STZ (50 mg/kg) followed by i.p. injections of oxidovanadium (IV)-orotate (40 mg/kg) every other day for 30 days (15 total treatments)

The animals were monitored daily and weighed weekly during the month-long study.

2.4.1. Chemical Induction of Diabetes. Animals fasted for 18 hours prior to receiving a single i.p. injection of STZ (50 mg/kg) that was freshly prepared in cold 0.1 M citrate buffer (pH 4.5). The STZ-injected animals were given a 5% glucose solution to drink *ad libitum* for the first 24 hours after injection to ensure survival [24]. Animals were considered as "diabetic" when their blood glucose levels exceeded 220 mg/dL, which occurred approximately 72 hours after STZ injection.

2.4.2. Blood and Tissue Collection. On day 30, after an 18-hour fast, blood samples were collected from the medial retroorbital venous plexus of the animals using capillary tubes (Micro Haematocrit Capillaries, Mucaps) under ether-induced anesthesia [25]. Approximately 3 mL of blood was collected from each animal and divided into two tubes, one of which contained EDTA (for use in hematological assays), while the other clotted for 30 minutes at room temperature prior to centrifugation at 3,000 rpm for 15 minutes to separate the serum (for use in biochemical analyses). The animals were then dissected under ether-induced anesthesia and tissue samples (liver and pancreas) were collected and washed with 1.15 % KCl and 0.5 mM EDTA. All samples were stored at -20°C until further analysis.

2.4.3. Insulin and Blood Glucose Levels. Insulin levels were determined as described by Woodhead *et al.* (1974) using the Insulin-I125 Kit and the Radioimmunoassay Kit (Radioassay System Laboratories Inc., England) [26]. Blood glucose levels were measured using the Udind Spain React Kit. Briefly, 10 μL of serum was incubated with 1 mL of the provided working reagent at 37°C for 10 minutes after which the developed colors were measured photometrically at 450 nm using a Biosystem 320 spectrophotometer relative to a tube filled only with the working solution. Glucose concentration was calculated according to the manufacturer's instructions.

2.4.4. Lipid Profiles. Total cholesterol (TC), triglyceride (TG), high-density lipoprotein cholesterol (HDL-c), and low-density lipoprotein cholesterol (LDL-c) levels were determined using fully autochemistry Integra 400 Plus Analyzer (Roche).

2.4.5. Glucose-6-Phosphate Dehydrogenase (G6PD) Activity. Glucose-6-phosphate dehydrogenase (G6PD) activity was measured using a commercially available kit.

2.4.6. Blood Superoxide Dismutase (SOD) Activity. Blood SOD activity was determined using a diagnostic kit according to manufacturer's instructions.

2.4.7. Liver and Kidney Function. The levels of ALT, creatinine, and uric acid were determined using autochemistry Integra 400 Plus Analyzer.

2.4.8. Hemoglobin (Hb) Levels. The Hb content (g/dL) of the blood was measured using a cell counter (Sysmex, Model KX21N).

2.4.9. Lactate Dehydrogenase (LDH) Activity. LDH activity was determined using a diagnostic kit according to manufacturer's instructions.

2.4.10. Histopathological Examination. Samples of the liver and pancreas were collected directly after dissection and immediately transferred to a 10% formalin solution for fixation. After 24 hours, the tissue samples were washed, dehydrated in ascending grades of alcohol, cleared in xylol, and embedded in paraffin. The paraffin blocks were cut into 5 um sections using a microtome. Prior to staining with Harris' hematoxylin and eosin (H & E), the paraffin was removed from the sections using xylene. After staining, the sections were dehydrated in alcohol, cleared with xylene, and mounted using Canada balsam [27].

2.5. Statistical Analyses. Data were reported as mean ± standard error of the mean (S.E.M.) for all groups (each group was considered as one experimental unit). Differences between groups were determined using the one-way analysis of variance (ANOVA) test (F-test) and, when significant differences between the means were found, Duncan's multiple range test. Statistical analyses were performed using the SPSS v15.0 software and p-values < 0.05 were considered reflective of statistical significance [28].

3. Results and Discussion

3.1. Interpretations of the Chemical Structure. The synthesized solid oxidovanadium (IV)-orotate complex was dark green,

Table 1: EPR spectral data of the oxidovanadium (IV)-orotate complex.

$g_\perp$	$g_\parallel$	g_{av}	$A_\parallel$ (cm^{-1})	$A_\perp$ (cm^{-1})	ΔB (G)
1.6719	1.5186	1.5952	78	71	1000

$*A_\parallel$ and$A_\perp$ = hyperfine constants; ΔB= full width at half maximum

is air stable, nonhygroscopic, soluble in DMSO and DMF solvents, and insoluble in water and most organic solvents, Figure 2. The physical and analytical data revealed a 1: 1 molar ration of VO(IV):OAH_3.

3.1.1. Microanalytical and Physical Data. Microanalytical data based on its chemical formula ($C_5H_{14}N_4O_8V$) predicted a molecular mass of 309 g/mol composed of (calculated) C = 19.41%, H = 4.53%, N = 18.12%, and V = 16.50%, which was in good agreement with the observed data: C = 19.33%, H = 4.48%, N = 18.04%, and V = 16.39%. Overall, the experimental values are compatible with the suggested formula $[(OAH_1)(VO)(NH_3)_2].3H_2O$ complex.

This dibasic oxidovanadium (IV)-orotate complex was isolated with a 70% yield and exhibited a melting point above 260°C. The molar conductivity of the complex in DMSO (10^{-3} M) was found to be 21 $\Omega^{-1}.cm^2.mol^{-1}$ at room temperature, which further highlighted its nonelectrolytic nature [29]. These results matched the elemental analysis data, where the absence of the SO_4^{2-} ion was confirmed using $BaCl_2.2H_2O$.

3.1.2. Electronic and Magnetic Measurements. The absorption bands observed around 16,000-16,529 cm^{-1} were due to the $^2B_2 \longrightarrow {}^2E$ and $^2B_2 \longrightarrow {}^2B_1$ electronic transitions [30]. The two weak bands at 19,048 and 23,809 cm^{-1} were assigned to the ligand-metal charge transfer (LM_{CT}). Magnetic moment of the A reference is afforded for the statement "2.20 BM that is attributed to square pyramidal geometry."

3.1.3. Electronic Paramagnetic Resonance (EPR) Spectrum. The EPR spectrum of the oxidovanadium (IV)-orotate complex was determined in DMSO at room temperature. The experimental data describing the $g_\parallel$ and $g_\perp$ factors aligned with other square pyramidal oxidovanadium (IV) complexes [31]. The $g_\parallel$, $g_\perp$, $A_\parallel$, and $A_\perp$ values were calculated from the spectra (Table 1) and the trends of the g values ($g_\parallel < g_\perp < 2$) were also concordant with square pyramidal structures.

3.1.4. Infrared Spectra. The essential bands from the infrared spectra of OAH_3 and its oxidovanadium (IV) complex are summarized in Table 2. Investigating the complex and free ligand separately enables investigation into the bonding patterns of the complex.

A comparison of the IR spectra of the free OAH_3 ligand and its oxidovanadium (IV) complex illuminated the following.

(I) the spectra of the solid complex exhibited broad bands in the 3450-3180 cm^{-1} regions, which may be attributed to ν(OH) of the coordinated water molecules and supported by bands in the ~830 range due to the rocking vibration motion $\delta_r(H_2O)$ of the coordinated water molecules.

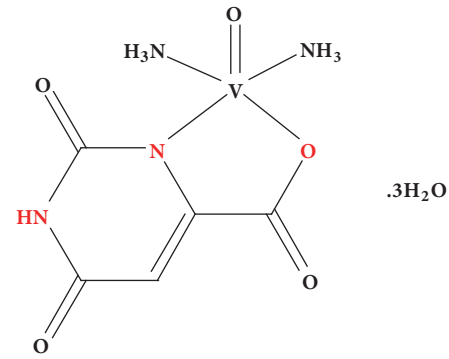

Figure 2: Proposed structure of the diammine-orotato-oxidovanadium (IV)complex.

(II) The ν(NH) bands at 3100 and 3003 cm^{-1} showed dramatic changes in position and intensity, which would suggest that at least one of the amino groups of the pyrimidine ring participates in bond formation with the oxidovanadium (IV) metal ions (Figure 3).

(III) The position and intensity of the strong bands of the carbonyl groups ν (C_{acidic}=O), ν(C_2=O), and ν(C_4=O) were shifted and broadened with respect to free OAH_3 [32]. It was found that C=O stretching bands situated adjacent to N-M will be greatly affected.

(IV) The $\delta(N_1H)$ band at 1516 cm^{-1} almost disappeared in the spectra of the complex suggesting that the N_1H group participates in binding with the metal ion through deprotonation. However, the $\delta(N_3H)$ band was almost unchanged, which confirms that the N_3H group does not participate in the coordination.

(V) The band at 3179 cm^{-1} in the $[(OA)(VO)(NH_3)_2].3H_2O$ complex can be assigned to the $\nu(NH_3)$ stretching vibrations, supported by a similar assignment at 3190 $cm^{-1}$for $[Ni(NH_3)_6]Cl_2$ [33]. The asymmetric deformation vibrations, $\delta(NH_3)$, probably overlap with the ν(C=O) transitions and H_2O bending vibrations. In the spectrum of studied complex, the $\nu(OH_{acid})$ band at 2633 cm^{-1} in the free ligand completely disappeared and a new carboxylate band νCOO appeared in the range of 1408-1405 cm^{-1}, which corresponded to $\nu_{as}(COO^-)$. The other band exhibited within the range of 1116-1112 cm^{-1} was assigned to $\nu_s(COO^-)$, indicating that the carboxylic group of OAH_3 participates in the coordination with the oxidovanadium (IV) ions through deprotonation. Moreover, the differences between the asymmetric and symmetric stretches of the carboxylate groups of the complexes, $\Delta\nu$ >200 cm^{-1}, suggest a monodentate binding of the carboxylate group to the metal ion [33]. The ν(V=O) vibration in the orotate complex was observed as expected as

Table 2: IR frequencies (cm^{-1}) of OAH_3 and the ammonium oxidovanadium (IV)-orotate complex.

Assignments	Compounds	
	OAH_3	$[(OA)(VO)(NH_3)_2].3H_2O$
ν(O-H); COOH and H_2O	3432	3410
ν(N1-H)	3100	--
ν(N3-H)	3003	3007
ν(N-H); NH_3	--	3179
ν(O-H); acid hydrogen bond	2633 2562 2491	--
ν(C=O); acid + ν(C2=O)	1706	1741
ν(C4=O) + ν(C=C)	1649	1679
$\nu_{as}(COO^-)$	--	1405
$\nu_s(COO^-)$	--	1113
$\delta(NH_3)$	--	1425
δ(N1H)	1516	--
δ(N3H)	1437	1433
ν(V=O)	--	933
ν(M-O)	--	543
ν(M-N)	--	429

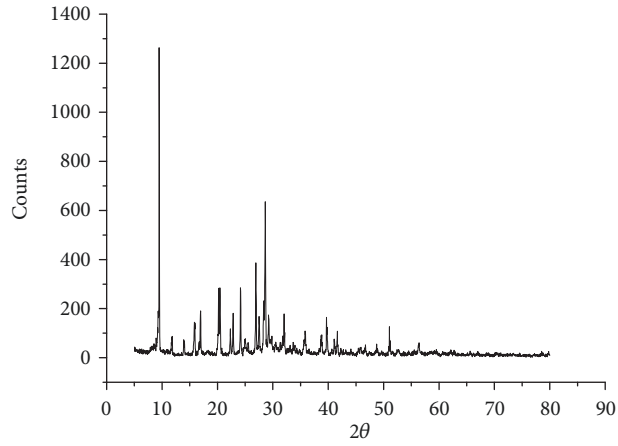

Figure 3: XRD of the solid oxidovanadium (IV)-orotate complex.

a strong band at 933 cm^{-1}, which is in good agreement with those known for many oxovanadium (IV) complexes [33]. In the far IR spectrum of oxidovanadium (IV) complex, new bands observed at 543 and 429 cm^{-1}can be assigned to the ν(M-O) and ν(M-N), respectively [33].

3.1.5. Thermal Analysis and Kinetic Thermodynamic Studies. The four-step thermal decomposition of the solid $[(OA)(VO)(NH_3)_2].3H_2O$ complex was investigated using thermogravimetry (TG, DTG, and DTA). These four degradation steps took place at temperature ranges 47-262°C, 262-387°C, 387-492°C, and 492-800°C, with DTG_{max} = 50, 327, 436, and 565°C, respectively. The experimental mass losses of these thermal decomposition steps are 17.20, 20.19, 14.70, and 13.91% which agree with theoretical values (17.47, 19.41, 14.23, and 14.23%), respectively, corresponded to losses $3H_2O$ molecules ($2NH_3$ gas + C_2H_2), CO_2 gas, and (N_2 + (1/2)O_2 gases) consequently. VO_2 + 2C was the final remaining residue, still stable at 800°C.

The calculated kinetic parameter values of ΔE∗, ΔA∗, ΔS∗, ΔH∗, and ΔG∗ for the decomposition steps of the $[(OA)(VO)(NH_3)_2].3H_2O$ complex are listed in Table 3 based on Coats-Redfern and Horowitz-Metzger relations [34, 35]. (I) The high activation energy of the oxidovanadium (IV)-orotate complex, reflected by the high ΔE∗ values of its decomposition, conferred thermal stability. (II) The negative ΔS∗ value of the decomposition suggests that the thermodynamic behavior of the oxidovanadium (IV)-orotate complex is nonspontaneous and more ordered.

3.1.6. Morphological Studies (XRD, SEM, and TEM). The XRD powder diffraction patterns of solid $[(OA)(VO)(NH_3)_2].3H_2O$ complex were scanned within the 2θ = 4-80° range (Figure 3). The resulting data were indicators of the crystallinity and purity of the solid-state compound. The XRD pattern generated by the oxidovanadium (IV)-orotate complex contained the peaks characteristic of vanadium metal at 41.61, 59.21, and 70.09, according to JCPDS File 22-1058 [36], and of OAH_3(9.54, 11.80, 13.85, 15.73, 16.87, 20.43, 22.86, 24.17, 26.97, 28.67, 32.04,35.79, 38.78, 45.72, 46.67, 48.72, 50.98, 52.46, and 56.21) within 2 θ = 4 -80°. The particle size of the oxidovanadium (IV)-orotate complex was estimated using the Scherrer equation [37] and the particle size from the highest diffraction peak was observed at 9.54°. The XRD pattern of the oxidovanadium (IV)-orotate complex indicated that it conformed to a nanocrystalline state and its particles were 5.00 nm in size.

The SEM micrographs captured at different magnifications showed that the oxidovanadium (IV)-orotate complex has cube-shaped particles (Figure 4(a)). Increasing

Table 3: Thermal decomposition of the oxidovanadium (IV)-orotate complex.

Method	Parameter					r
	E ($J\ mol^{-1}$)	A (s^{-1})	ΔS ($J\ mol^{-1}K^{-1}$)	ΔH ($J\ mol^{-1}$)	ΔG ($J\ mol^{-1}$)	
CR	1.86E+05	2.74E+11	-3.31E+01	1.80E+05	2.03E+05	0.9967
HM	1.95E+05	2.78E+12	-1.39E+01	1.89E+05	1.99E+05	0.9997

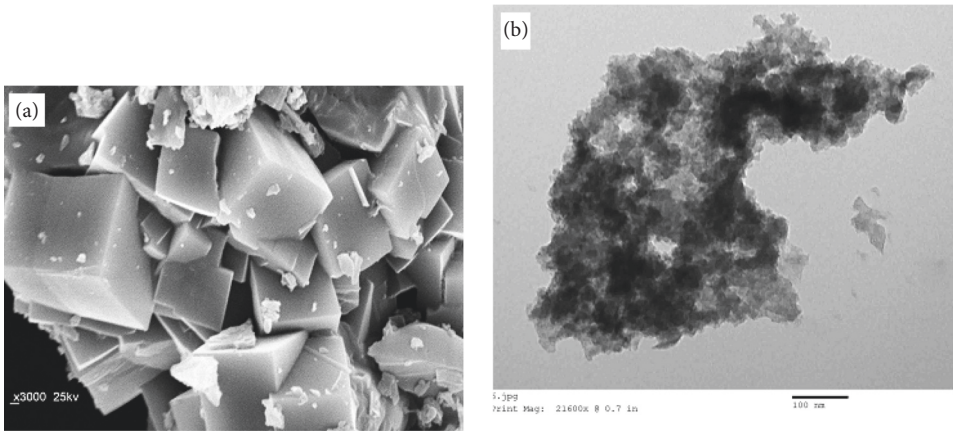

Figure 4: Electron microscopy images of the solid oxidovanadium (IV)-orotate complex. (a) SEM image (b) TEM micrograph.

the magnification afforded better resolution of the distinct particles. The TEM images revealed that the particles of the $[(OA)(VO)(NH_3)_2].3H_2O$ complex varied in size (average: 5 nm) and were irregularly shaped (Figure 4(b)).

3.2. In Vivo Application of the Oxidovanadium (IV)-Orotate Complex

3.2.1. Blood Glucose and Insulin Levels. The levels of blood glucose and insulin are presented in Table 4. STZ has been used extensively to produce an experimental animal model of diabetes because it is selectively toxic to β cells in the pancreatic islets. The i.p. injection of oxidovanadium (IV) sulfate alone (Group III: 283.51 ± 9.21 mg/dL) and the oxidovanadium (IV)-orotate complex (Group IV: 410.23 ± 14.52 mg/dL) both significantly decreased blood glucose levels relative to the STZ-treated positive control (Group II: 273.77 ± 5.11 mg/dL). This effect was slightly more pronounced in Group IV than in Group III. In line with our results, many studies have shown that the administration of vanadate or oxidovanadium (IV) essentially normalizes the pathological effects of STZ treatment thereby restoring normoglycemia [38].

The healthy control animals had significantly higher insulin levels than their diabetic counterparts (Group I: 57.64 ± 1.76 IU/mL, Group II 23.78 ± 2.50 IU/mL). These untreated diabetic animals had significantly less insulin than those treated for 30 days with either oxidovanadium (IV) sulfate alone (Group III: 41.44 ± 1.23IU/mL) or the oxidovanadium (IV)-orotate complex (Group IV: 42.67 ± 1.77 IU/mL). These findings support reports in the literature that oxidovanadium(IV) salts can mimic many of the metabolic actions of insulin both *in vitro* and *in vivo* and improve the glycemic control that is lacking in diabetes [39–41].

3.2.2. Lipid Profile. The levels of TC, TG, HDL-c, and LDL-c are presented in Table 4. The results indicate that the levels of TC, TG, and LDL-c were significantly increased in the STZ-induced diabetic animals (Group II) compared to the healthy controls (Group I). This is in contrast to data published by Butt et al. (2002) that showed a reduction in serum HDL-c levels in STZ-induced diabetic animals [42]. High levels of serum lipids in diabetes are mainly caused by the increased mobilization of free fatty acids from their peripheral stores because insulin inhibits hormone-sensitive lipases. The excess fatty acids are converted into phospholipids and cholesterol in the liver. The degree of hypercholesterolemia is directly proportional to severity in diabetes. The liver is an insulin-dependent tissue that plays a crucial role in glucose and lipid homeostasis that is severely affected by diabetes. Diabetes results in decreased glucose utilization and increased glucose production in insulin-dependent tissues, such as the liver. The present study showed that the administration of the oxidovanadium (IV) complex (Group IV) led to significantly decreased TC, TG, and LDL-c (38.03%, 23.26%, and 26.89%, respectively) while HDL-c levels were significantly increased (40.78%) relative to the diabetic control (Group II). The underlying mechanism by which oxidovanadium (IV) sulfate exerts its cholesterol-lowering effect seems to be a decrease in cholesterol absorption from the intestine, by binding to bile in the intestine and increasing its excretion [43]. However, oxidovanadium (IV) sulfate also decreases cholesterol biosynthesis, specifically by reducing 3-hydroxy-3-methylglutaryl-CoA (HMG-CoA)

Table 4: Biochemical effects of the oxidovanadium (IV)-orotate complex *in vivo*.

Molecule of interest	Group I	Group II	Group III	Group IV
Insulin (IU/mL)	57.64±1.76	23.78±2.50	41.44±1.23	42.67±1.77
Glucose (mg/dL)	77.55±4.93	410.23±14.52	283.51±9.21	273.77±5.11
GPT (U/L)	72.33±7.43	111.50±8.39	124.31±9.66	106.45±4.95
Creatinine (mg/dL)	0.52±0.12	1.14±0.18	0.85±0.15	0.77±0.13
Uric acid (mg/dL)	3.52±0.24	4.79±0.37	3.86±0.29	3.81±.28
LDH (U/L)	295.43±15.33	409.55±13.27	434.72±19.76	390.41±14.22
G6PD (U/L)	12.13±0.64	7.92±0.47	9.25±.41	10.13±0.41
Hb(g/dL)	12.82±.44	9.83±0.37	10.85±0.51	11.39±0.61
SOD (U/mL)	307.53±15.15	259.41±21.66	280.37 ±18.76	281.65±17.55
TC (mg/dL)	75.66±7.65	210.52±10.57	129.66±8.77	127.48±5.69
TG(mg/dL)	139.67±9.45	197.46±11.86	156.77±10.56	154.43±9.34
HDL-c (mg/dL)	42.33±3.12	21.44±1.77	32.32±2.11	34.43±3.22
LDL-c (mg/dL)	31.33±4.22	52.57±5.32	42.88±4.71	39.33±4.32

reductase activity, a key enzyme in cholesterol biosynthesis, and/or by reducing the NADPH required for fatty acid and cholesterol biosynthesis [32, 43]. In addition, oxidovanadium (IV) may improve hypercholesterolemia by modulating lipoprotein metabolism: enhancing LDL uptake by increasing LDL receptor expression [32] and/or by increasing lecithin cholesterol acyltransferase activity [44]. Overall, these results indicate that treatment with the complex developed in this study could help combat the diverse metabolic issues associated with diabetes beyond glucose metabolism.

3.2.3. Glucose-6-Phosphate Dehydrogenase (G6PD) Activity. G6PD is the principal source of the intracellular reductant NADPH, which is required by many enzymes including those of the antioxidant pathway [44]. G6PD deficiency is associated with diabetes, yet the nature of their relationship remains unclear. The level of G6PD decreased in all of the diabetic animals compared to the healthy control animals (Table 4), as has been previously reported [44]. Treatment with the oxidovanadium (IV)-orotate complex (Group IV: 10.13 ± 0.41 U/L) significantly increased G6PD activity by 15.74% relative to the diabetic group (Group II: 7.92 ± 0.47 U/L), whereas treatment with oxidovanadium (IV) sulfate alone increased activity by 14.37% (Group III: 9.25 ± 0.41 U/L).

3.2.4. Superoxide Dismutase (SOD) Activity. SOD is a major component of the antioxidant system that neutralizes superoxide radicals by converting them into H_2O_2 and molecular oxygen. SOD activity is decreased in patients with diabetes, which is likely due to the saturation of this enzyme with the free radicals induced by the disease [41]. As expected, SOD activity decreased significantly in the diabetic animals (Group II: 259.41 ± 21.66 U/mL) compared to the healthy controls (Group I: 307.53 ± 15.15U/mL). There was a decrease in the diabetic group treated with the oxidovanadium (IV)-orotate complex (Group IV: 281.65 ± 17.55 U/mL) and a decrease in the group treated with oxidovanadium (IV) sulfate alone (Group III: 280.37 ± 18.76U/mL). The increased SOD activity induced by oxidovanadium (IV) complex treatment would help manage the elevated free radicals associated with diabetes.

3.2.5. Liver and Kidney Function. Serum GPT is the major enzyme used to determine liver function since it is released upon liver cell damage [43]. The activity of the GPT enzyme in the different experimental groups is presented in Table 4. The results indicated that the injection of oxidovanadium (IV) sulfate alone slightly increased the activity of the GPT enzyme from 111.50 ± 8.39 U/L in Group II to 124.31 ± 9.66 U/L in Group III, while the injection of the oxidovanadium (IV)-orotate complex decreased serum GPT activity in Group IV to 106.45 ± 4.95 U/L, which is less than Group II and less than Group III. These results indicate that treatment with the oxidovanadium (IV)-orotate complex had little effect on liver cells compared to STZ or oxidovanadium (IV) alone, but all three had much higher levels than Group I (72.33 ± 7.43 U/L). These data suggest that the oxidovanadium (IV)-orotate complex is less toxic than oxidovanadium (IV) sulfate alone.

Serum creatinine is an important measure of the viability and health of the kidney: increasing creatinine levels are indicative of kidney failure and this parameter is highly elevated in diabetics [32]. According to the results shown in Table 4, this pathological feature of diabetes was nicely recapitulated in the animal model used in this study, as creatinine levels in the diabetic rats (Group II: 1.14 ± 0.18 mg/dL) were over twice those of the healthy controls (Group I: 0.52 ± 0.12 mg/dL). The treatment with oxidovanadium (IV) sulfate alone (Group III: 0.85 ± 0.15 mg/dl) and the oxidovanadium (IV)-orotate complex (Group IV: 0.77 ± 0.13 mg/dL) decreased creatinine levels compared to the untreated diabetic rats in Group II. While the reduction was more pronounced in Group IV than in Group III, the difference between these two experimental groups was not statistically significant. These data indicate that neither oxidovanadium (IV) nor its orotate complex had a major effect on kidney tissue *in vivo* and greatly improved kidney function.

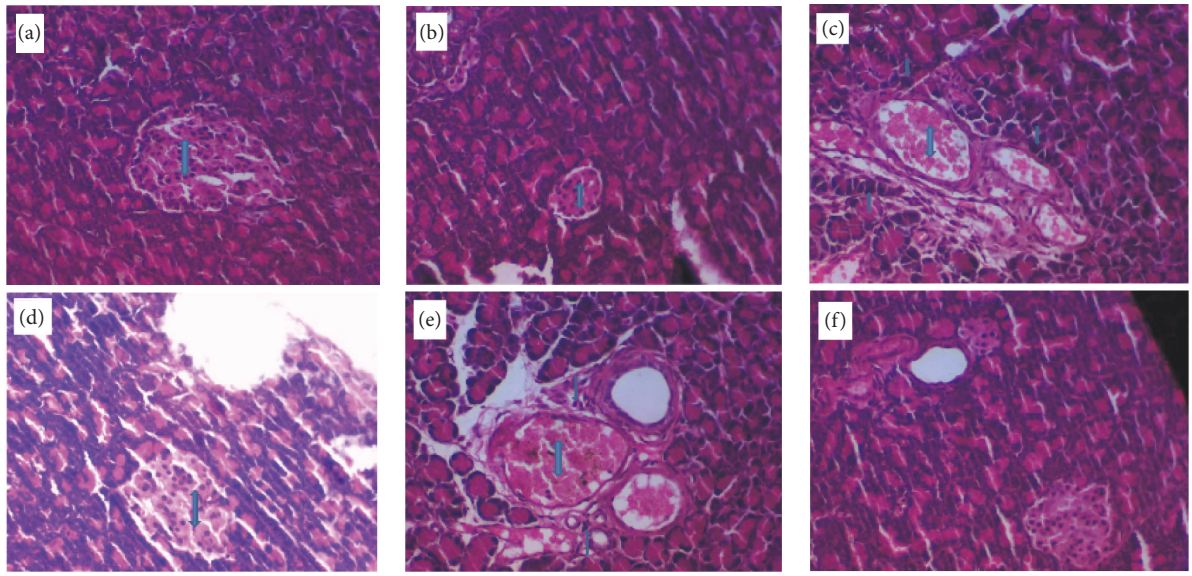

Figure 5: Histology of the pancreas. Pancreatic tissue was collected from each animal after 30 days of treatment. The tissue was sectioned, stained using H & E, and imaged using standard light microscopy at 400 x magnifications. Double-sided arrows (↕) denote an islet of Langerhans. (a) Pancreas from healthy control animal (Group I), (b,c) Pancreas from STZ-treated diabetic animal (Group II), (d,e) Pancreas from animal treated with oxidovanadium(IV) sulfate alone (Group III), (f) Pancreas from animal treated with oxidovanadium (IV)-orotate complex (Group III).

The increase in uric acid levels (hyperuricemia) observed in the diabetic rats (Group II: 4.79 ± 0.37 mg/dL) relative to the healthy controls (Group I: 3.52 ± 0.24mg/dL) was consistent with that reported in a previous study [44]. Compared to Group II, uric acid levels decreased by 20.5% after 30 days of oxidovanadium (IV)-orotate treatment (Group IV: 3.81 ± 0.28 mg/dL) and with oxidovanadium (IV) alone (Group III: 3.86 ± 0.29 mg/dL). This reduction can be explained by the inhibition of oxidative phosphorylation, which leads to a decrease in protein synthesis [43].

3.2.6. Lactate Dehydrogenase (LDH) Activity. LDH is used as a marker of tissue breakdown as this enzyme is abundant in red blood cells and is released upon hemolysis [44]. The activity of the LDH enzyme in the different experimental groups is presented in Table 4. The activity of serum LDH in the diabetic positive control animals (Group II: 409.55 ± 13.27 U/L) was significantly increased relative to the healthy control group (Group I: 295.43 ± 15.33 U/L). The administration of the oxidovanadium (IV)-orotate complex (Group IV: 390.41 ± 14.22 U/L) elicited a 5% decrease in LDH activity compared to Group II. In contrast, treatment with oxidovanadium (IV) sulfate alone (Group III: 434.72 ± 19.76 U/L) resulted in an even greater activity increase than observed in the positive control. The LDH activity in this animal model of diabetes mainly reflects the leakage of LDH into the bloodstream caused by STZ toxicity in the liver.

3.2.7. Hemoglobin (Hb) Levels. Hb is the iron-containing oxygen-transporting metalloprotein in red blood cells that carries oxygen from the respiratory organs to the rest of the body. The reduction of Hb and the ensuing anemia associated with diabetes were largely caused by the increased nonenzymatic glycosylation of red blood cell membrane proteins [40]. Oxidation of these proteins and hyperglycemia in diabetes increases the production of lipid peroxides thereby causing hemolysis and other pathological consequences. The levels of Hb in the different experimental groups are presented in Table 4. Results indicated that Hb levels decreased in the diabetic rats (Group II: 9.83 ± 0.37 g/dL) compared to the healthy animals (Group I: 12.82 ± 0.44 g/dL). The administration of the oxidovanadium (IV)-orotate complex increased serum Hb content by 13.70% at the study's 30-day endpoint (Group IV: 11.39 ± 0.61 g/dL) compared to the untreated diabetic group, while oxidovanadium (IV) sulfate alone increased Hb (Group III: 10.85 ± 0.51 g/dL).

3.2.8. Histopathology of the Pancreas. Cells of the pancreas from the healthy control animals (Group I) were present in their expected proportions and structures, including typically sized islet of Langerhans surrounded by healthy pancreatic acini (Figure 5(a)). On the other hand, the pancreatic tissues in the STZ-treated diabetic animals (Group II) exhibited atrophy of the islet of Langerhans and dilated congested vascular spaces surrounded by aggregates of inflammatory cells and pancreatic acini (Figure 5(b)). The islets were largely occupied by eosinophilic material and reduced in size (Figure 5(c)). Eosinophilic material also surrounded the blood vessels, as indicated in Figures 5(b) and 5(c). The pancreatic tissue from diabetic animals treated with oxidovanadium (IV) sulfate alone (Group III) showed a slight increase in the size of the islet of Langerhans compared to Group II and dilated, congested vascular space surrounded by aggregates of inflammatory cells (Figure 5(d)). The pancreatic tissues from diabetic animals treated with the oxidovanadium (IV)-orotate complex had moderately increased islet of Langerhans

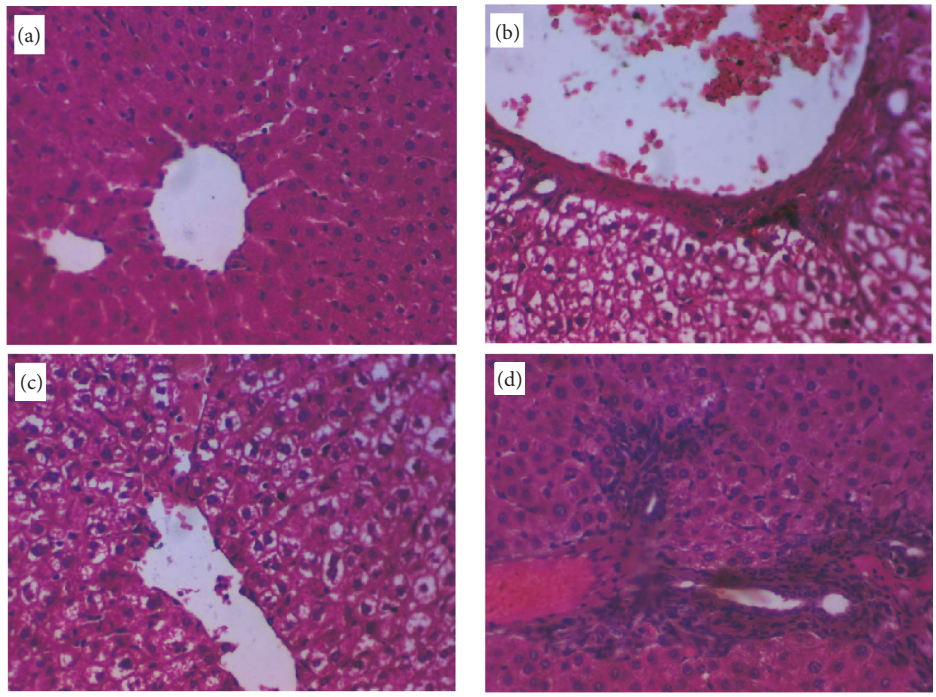

Figure 6: Histology of the liver. Liver tissue was collected from each animal after 30 days of treatment. The tissue was sectioned, stained using H & E, and imaged using standard light microscopy at 400 x magnifications. Double-sided arrows (↕) denote the central vein and single-sided arrows (↑) indicate hepatocytes. (a) Liver from healthy control animal (Group I), (b) Liver from STZ-treated diabetic animal (Group II), (c) Liver from animal treated with oxidovanadium(IV) sulfate alone (Group III), (d) Liver from animal treated with the oxidovanadium(IV)-orotate complex (Group IV).

surrounded by healthy-looking pancreatic acini and acinar cells and very few infiltrating inflammatory cells (Figure 5(f)).

3.2.9. Histopathology of the Liver. Microscopically, the liver tissue from the healthy control animals (Group I) contained healthy substructures, including typical central vein morphology and rows and cords of healthy hepatocytes with central nuclei and blood sinusoids (Figure 6(a)). On the other hand, the liver tissue from the diabetic control rats (Group II) showed large areas of hepatic necrosis with a markedly dilated congested central vein filled with red blood cells, rows and cords of swollen and degenerating hepatocytes with severe fatty changes, and inflammatory cell infiltration (Figure 6(b)). Compared to Group II, the liver tissues from the diabetic animals treated with oxidovanadium (IV) sulfate alone (Group III) showed improvement in the degree of hepatic necrosis with an only partially dilated congested central vein, decreased fatty changes to the hepatocytes, and less inflammatory cell infiltration (Figure 6(c)). The liver tissues from the diabetic animals treated with the oxidovanadium (IV)-orotate complex exhibited even greater improvement compared to Group II including further reduction in the congestion and dilation of the central vein and fewer inflammatory cells (Figure 6(d)).

4. Conclusion

In the present study, new antidiabetic drug titled as diammine-orotato-oxidovanadium (IV), $[(OAH_1)(VO)(NH_3)_2].3H_2O$, complex has been designed in neutralized media by the 1:1 chemical reaction between orotic acid (OAH_3) and oxidovanadium (IV) sulfate. Spectroscopic approach is used to determine and confirm the chemical structure of this complex like UV-visible spectroscopy, ^{1}H NMR spectroscopy, FT-IR spectroscopy, electron spin resonance (EPR), thermogravimetric (TG), differential thermogravimetric (DTG), differential thermal (DTA), scanning electron microscopy (SEM), transmission electron microscopy (TEM), and X-ray diffraction patterns. The antidiabetic efficiency was evaluated against streptozocin-induced diabetes in male albino rats. The insulin hormone and blood glucose level, lipid profile, liver and kidney functions, and superoxide dismutase antioxidant (SOD) are qualified factors to identify the efficiency of diammine-orotato-oxidovanadium (IV) complex as an alternative antidiabetic drug model.

Data Availability

The data used to support the findings of this study are available from the corresponding author upon request.

Conflicts of Interest

All authors declare that there are no conflicts of interest regarding the publication of this article.

Authors' Contributions

Ahmed M. Naglah and Moamen S. Refat are equal contributing authors.

Acknowledgments

The authors would like to extend their sincere appreciation to the Deanship of Scientific Research at King Saud University for its funding of this research through the Research Group No.: RG-1436-015.

References

[1] W. M. Kwiatek, T. Drewniak, M. Gajda, M. Gałka, A. L. Hanson, and T. Cichocki, "Preliminary study on the distribution of selected elements in cancerous and non-cancerous kidney tissues," *Journal of Trace Elements in Medicine and Biology*, vol. 16, no. 3, pp. 155–160, 2002.

[2] M. Gielen and E. R. T. Tiekink, *Metallotherapeutic Drugs and Metal-Based Diagnostic Agents, the Use of Metals in Medicine*, Wiley, Chichester, UK, 2005.

[3] S. K. Bharti and S. K. Singh, "Metal Based Drugs: Current Use and Future Potential," *Der Pharmacia Lettre*, vol. 1, pp. 39–51, 2009.

[4] J. E. Weder, C. T. Dillon, T. W. Hambley et al., "Copper complexes of non-steroidal anti-inflammatory drugs: an opportunity yet to be realized," *Coordination Chemistry Reviews*, vol. 232, no. 1-2, pp. 95–126, 2002.

[5] D. C. Ware, P. J. Brothers, G. R. Clark, W. A. Denny, B. D. Palmer, and W. R. Wilson, "Synthesis, structures and hypoxia-selective cytotoxicity of cobalt(III) complexes containing tridentate amine and nitrogen mustard ligands," *Journal of the Chemical Society, Dalton Transactions*, no. 6, pp. 925–932, 2000.

[6] M. Nakai, F. Sekiguchi, M. Obata et al., "Synthesis and insulin-mimetic activities of metal complexes with 3-hydroxypyridine-2-carboxylic acid," *Journal of Inorganic Biochemistry*, vol. 99, no. 6, pp. 1275–1282, 2005.

[7] F. Ghasemi, A. R. Rezvani, K. Ghasemi, and C. Graiff, "Glycine and metformin as new counter ions for mono and dinuclear vanadium(V)-dipicolinic acid complexes based on the insulin-enhancing anions: Synthesis, spectroscopic characterization and crystal structure," *Journal of Molecular Structure*, vol. 1154, pp. 319–326, 2018.

[8] X. Yang, "Biology of Vanadium-Based Compounds for Treatment of Diabetes," *Reference Module in Chemistry, Molecular Sciences and Chemical Engineering*, 2018.

[9] M. S. Adam and H. Elsawy, "Biological potential of oxo-vanadium salicylediene amino-acid complexes as cytotoxic, antimicrobial, antioxidant and DNA interaction," *Journal of Photochemistry and Photobiology B: Biology*, vol. 184, pp. 34–43, 2018.

[10] S. Roy, S. Mallick, T. Chakraborty et al., "Synthesis, characterisation and antioxidant activity of luteolin-vanadium(II) complex," *Food Chemistry*, vol. 173, pp. 1172–1178, 2015.

[11] M. Li, W. Ding, B. Baruah, D. C. Crans, and R. Wang, "Inhibition of protein tyrosine phosphatase 1B and alkaline phosphatase by bis(maltolato)oxovanadium (IV)," *Journal of Inorganic Biochemistry*, vol. 102, no. 10, pp. 1846–1853, 2008.

[12] A. K. Srivastava and M. Z. Mehdi, "Insulino-mimetic and anti-diabetic effects of vanadium compounds," *Diabetic Medicine*, vol. 22, no. 1, pp. 2–13, 2005.

[13] J. Victor, L. B. Greenberg, and D. L. Sloan, "Studies of the kinetic mechanism of orotate phosphoribosyltransferase from yeast.," *The Journal of Biological Chemistry*, vol. 254, no. 8, pp. 2647–2655, 1979.

[14] G. Maistralis, A. Koutsodimou, and N. Katsaros, "Transition metal orotic acid complexes," *Transition Metal Chemistry*, vol. 25, no. 2, pp. 166–173, 2000.

[15] H. Van Der Meersch, "Use of orotic acid and orotates," *Journal de Pharmacie de Belgique*, vol. 61, no. 4, pp. 97–104, 2006.

[16] P. Castan, S. Wimmer, E. Colacio-Rodriguez, A. L. Beauchamp, and S. Cros, "Platinum and palladium complexes of 3-methyl orotic acid: A route toward palladium complexes with good antitumor activity," *Journal of Inorganic Biochemistry*, vol. 38, no. 3, pp. 225–239, 1990.

[17] A. S. Hassan and J. A. Milner, "Alterations in liver nucleic acids and nucleotides in arginine deficient rats," *Metabolism*, vol. 30, no. 8, pp. 739–744, 1981.

[18] K. R. Geiss, N. Stergiou, Jester, H. U. Neuenfeld, and H.-G. Jester, "Effects of magnesium orotate on exercise tolerance in patients with coronary heart disease," *Cardiovascular Drugs and Therapy*, vol. 12, no. 2, pp. 153–156, 1998.

[19] G. K. Hinkel, H. W. Kintzel, and R. Schwarze, "Prevention of hyperbilirubinemia in premature and newborn infants using orotic acid," *Das Deutsche Gesundheitswesen*, vol. 27, no. 51, pp. 2414–2419, 1972.

[20] G. Muller, "Metabolic effects of orotic acid," *Zeitschrift für die gesamte innere Medizin und ihre Grenzgebiete*, vol. 39, no. 12, pp. 269–273, 1984.

[21] P. Collipp, "Orotic acid, inosine and nucleosides in the treatment of degenerative retinal diseases: a double blind study," *Current Therapeutic Research*, vol. 42, p. 235, 1987.

[22] W. N. Kelley and J. B. Wyngaarden, "Drug treatment of gout," *Seminars in Drug Treatment*, vol. 1, p. 119, 1971.

[23] L. Hounsom, D. F. Horrobin, H. Tritschler, R. Corder, and D. R. Tomlinson, "A lipoic acid-gamma linolenic acid conjugate is effective against multiple indices of experimental diabetic neuropathy," *Diabetologia*, vol. 41, no. 7, pp. 839–843, 1998.

[24] E. Hajduch, F. Darakhshan, and H. S. Hundal, "Fructose uptake in rat adipocytes: GLUT5 expression and the effects of streptozotocin-induced diabetes," *Diabetologia*, vol. 41, no. 7, pp. 821–828, 1998.

[25] S. H. Stone, "Method for obtaining venous blood from the orbital sinus of the rat or mouse," *Science*, vol. 119, no. 3081, p. 100, 1954.

[26] O. Woodhead, P. Otton, and L. Spake, "Radioimmunoassay of insulin," *Clinical Pharmacology*, vol. 21, pp. 11–15, 1974.

[27] H. M. Carleton, *Carleton's Histological Technique*, Oxford University Press, London, UK, NY, USA, Toronto, Canada, 4th edition, 1967.

[28] G. W. Snedecor and W. G. Cochran, *Statistical Methods*, Iowa State University Press, Ames, Iowa, USA, 8th edition, 1980.

[29] W. J. Geary, "The use of conductivity measurements in organic solvents for the characterisation of coordination compounds," *Coordination Chemistry Reviews*, vol. 7, no. 1, pp. 81–122, 1971.

[30] A. B. P. Lever, *Inorganic Electronic Spectroscopy*, Elsevier, Amsterdam, The Netherlands, 1986.

[31] M. Vlasiou, C. Drouza, T. A. Kabanos, and A. D. Keramidas, "Donor atom electrochemical contribution to redox potentials of square pyramidal vanadyl complexes," *Journal of Inorganic Biochemistry*, vol. 147, pp. 39–43, 2015.

[32] S. Rajasekaran, K. Sivagnanam, and S. Subramanian, "Mineral contents of Aloe vera leaf gel and their role on streptozotocin-induced diabetic rats," *Biological Trace Element Research*, vol. 108, no. 1-3, pp. 185–195, 2005.

[33] Z. M. Zaki, S. S. Haggag, and M. El-Shabasy, "Structural Chemistry of Some Imidazole Complexes," *Spectroscopy Letters*, vol. 28, no. 3, pp. 489–501, 1995.

[34] A. W. Coats and J. P. Redfern, "Kinetic parameters from thermogravimetric data," *Nature*, vol. 201, no. 4914, pp. 68-69, 1964.

[35] H. H. Horowitz and G. Metzger, "A new analysis of thermogravimetric traces," *Analytical Chemistry*, vol. 35, no. 10, pp. 1464–1468, 1963.

[36] A. Miyauchi and T. H. Okabe, "Production of metallic vanadium by preform reduction process," *Materials Transactions*, vol. 51, no. 6, pp. 1102–1108, 2010.

[37] B. D. Cullity, *Elements of X-ray Diffraction*, Addison-Wesley Publication Company, Massachusetts, USA, 1978.

[38] Y. Yoshikawa, E. Ueda, K. Kawabe et al., "Development of new insulinomimetic zinc(II) picolinate complexes with a Zn(N2O2) coordination mode: structure characterization, in vitro, and in vivo studies," *JBIC Journal of Biological Inorganic Chemistry*, vol. 7, no. 1-2, pp. 68–73, 2002.

[39] Braunwald, "Evaluation of liver function," in *Harrison's Principles of Internal Medicine*, E. Braunwald, Ed., pp. 1711–1715, McGraw-Hill, NY, USA, 2001.

[40] W. Ganong, *Review of Medical Physiology, Lange Medical Books*, vol. 13, McGraw-Hill, NY, USA, 2003.

[41] S. Ashakiran, N. Krishnamurthy, S. Navin, and S. Patil, "Behaviour of serum uric acid and lipid profile in relation to glycemic status in proliferative and non-proliferative diabetic retinopathy," *Current Neurobiology*, vol. 2, no. 1, pp. 57–61, 2011.

[42] A. A. Butt, S. Michaels, D. Greer, R. Clark, P. Kissinger, and D. H. Martin, "Serum LDH level as a clue to the diagnosis of histoplasmosis," *The AIDS Reader*, vol. 12, no. 7, pp. 317–321, 2002.

[43] T. Szudelski, "The Mechanism of Alloxan and Streptozotocin Action in B Cells of the Rat Pancreas," *Physiological Research*, vol. 50, pp. 537–546, 2001.

[44] L. Pari and M. Amarnath Satheesh, "Antidiabetic activity of *Boerhaavia diffusa* L.: effect on hepatic key enzymes in experimental diabetes," *Journal of Ethnopharmacology*, vol. 91, no. 1, pp. 109–113, 2004.